

even a slight fall along with a fall in the average thickness due to the breakaway δ_{ay} . At the same time, there is a marked reduction in the rate of fall in the average thickness of the continuous layer.

LITERATURE CITED

1. H. Brauer, "Strömung und Wärmeübergang bei Reifselfilmen," VDJ Forschungsheft, 457, No. 22 (1956).
2. E. G. Vorontsov, "Features of the wave flow variation with a path traveled in a film," Inzh.-Fiz. Zh., 16, No. 1, (1969).
3. B. G. Ganchev, V. M. Kozlov, and V. V. Lozovetskii, "A study of a descending flow of liquid on a vertical surface and the heat transfer to it," Inzh.-Fiz. Zh., 20, No. 4 (1971).
4. B. G. Ganchev, V. M. Kozlov, "A study of the gravitational flow of a film of liquid over the walls of a vertical channel of considerable length," Zh. Prikl. Mekh. Tekh. Fiz., No. 1, (1973).
5. K. J. Chu and A. E. Dukler, "Statistical characteristics of thin, wavy films. Pt III. Structure of the large waves and their resistance to gas flow," AIChE J., 21, No. 3 (1975).
6. B. G. Ganchev, V. M. Kozlov, and V. V. Lozovetskii, "Flow of a film of liquid in a vertical channel," in: Research on Processes in Power Systems, issue 2 [in Russian], Izd. MVTU, Moscow (1975).
7. L. N. Maurin and V. S. Sorokin, "Wave flow of thin layers of viscous liquid," Zh. Prikl. Mekh. Tekh. Fiz., No. 4 (1962).
8. V. E. Nakoryakov and I. R. Shreiber, "Waves at the surface of a thin layer of viscous liquid," Zh. Prikl. Mekh. Tekh. Fiz., No. 2 (1973).

AN EXPERIMENTAL STUDY OF INTERNAL SOLITARY WAVES IN A TWO-LAYER LIQUID

V. I. Bukreev and N. V. Gavrilov

UDC 552.593

Experimental data have been derived to check some theoretical results on internal solitary waves in two different cases. In the first, the solitary wave is generated at the interface between two thin layers of immiscible liquids with densities ρ_1 and $\rho_2 > \rho_1$, which are bounded below by a horizontal floor and above by a free surface, and which are at rest in the unperturbed state (Fig. 1a). This situation was first considered theoretically in the Boussinesq approximation in [1], and then under conditions where the Cortvega-de Brees equation applies in [2, 3].

Experimental studies corresponding to this case were performed in [4, 5]. The information obtained there has been supplemented in our studies, in particular in that in the experiments the paths of the liquid particles were recorded along with the speed of the solitary wave and the profile of this. Previously, two laboratory studies had been performed on internal solitary waves in a liquid at rest in the unperturbed state [6, 7], but with a depth distribution of the density different from that given above and with a different flow geometry.

In the second of these cases, the layers were bounded above by an impermeable horizontal cover, and, which is more important, there was a velocity shear between the layers in the unperturbed state (Fig. 1b). It was first predicted that solitary waves can occur at the interface in this case on the basis of the second approximation in shallow-water theory by Ovsyannikov, and this study will be mentioned below as in [8] (a brief abstract of the paper is mentioned in the literature list under this number).

In what follows we use immobile rectangular coordinate system x, y as shown in Fig. 1 (the different positions of the origin along the y axis and the different ways of specifying the depths in schemes a and b have been used for conformity with the corresponding theoretical studies). The deviation of the interface from the equilibrium position is denoted by η ,

Novosibirsk. Translated from Zhurnal Prikladnoi Mekhaniki i Tekhnicheskoi Fiziki, No. 5, pp. 51-56, September-October, 1983. Original article submitted July 23, 1982.

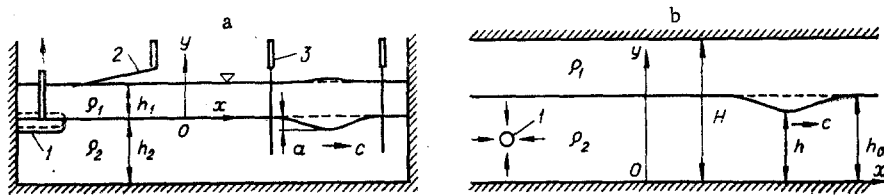


Fig. 1

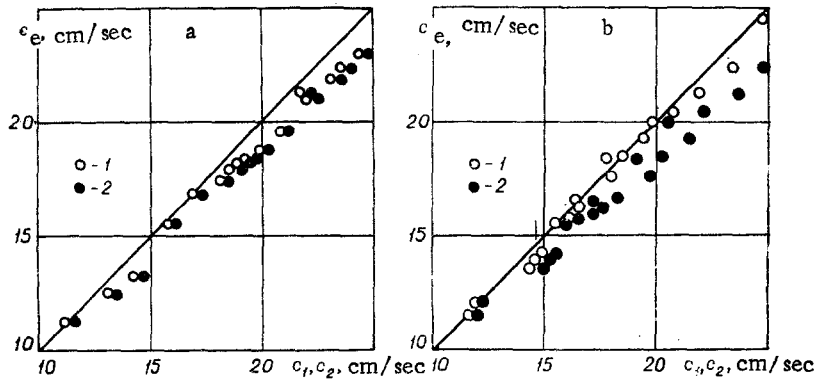


Fig. 2

and the maximum deviation (wave amplitude) by α , with the wave propagation speed c . We consider only two-dimensional waves.

To realize the scheme shown in Fig. 1a, we used a lucite trough of rectangular cross section and having a length of 220 cm, width 17 cm, and height 15 cm. The stratification was produced by means of one of two parts of immiscible liquids: kerosene and water with a density ratio $\sigma = \rho_1/\rho_2 = 0.8$ or water and khladone-113 with $\sigma = 0.67$. The solitary wave at the interface was generated as in [4, 5] by the plate 1, which was displaced a certain distance along the vertical. This produced an undesirable perturbation in the free surface, which in the theoretical analysis corresponds to the so-called fast mode of oscillation. In the experiments, these perturbations were small in intensity and were effectively damped out by the inclined plate 2. The waves were recorded by the conductivity transducers 3, which were made for these experiments by V. V. Zykov and E. I. Khakhilev, and also by photographic recording.

The scheme of Fig. 1b was implemented in a lucite trough, in which the lower liquid (water) could move with a speed u_0 uniformly distributed over the vertical in the initial section, while in the upper layer (kerosene) there was only a weak circulation due to the friction at the interface. The length of the working part was 100 cm, width 20 cm, and the height H was varied. The solitary wave with its convexity downwards was generated by withdrawing the water through a perforated tube shown as 1 in the figure, i.e., by the brief application of a sink uniformly distributed over the width of the trough. The solitary wave with its convexity upwards was generated similarly by switching on a source. The water flow rate was measured with an overflow having a sharp edge placed in the pipeline. This had previously been calibrated by the volumetric method. This apparatus was also used in experiments with layers at rest in the unperturbed state, but with an impermeable lid in place of the free surface as the upper boundary. In that case, the solitary waves were generated with a plate.

The metrological characteristics of the transducers were such that there was a linear static calibration curve with negligibly small hysteresis and with spatial and time resolution meeting the requirements. The random errors of measurement were represented by a coefficient of variation of not more than 5% and are illustrated by the spread in the points in the figures given below.

The basic difference in the conditions in these models was that in the latter ones no allowance was made for the effects of the viscosity in the real liquids. Also, at the interface there was surface tension, which was also not incorporated into the models. However, in this study the surface tension played only a positive part. It effectively sup-

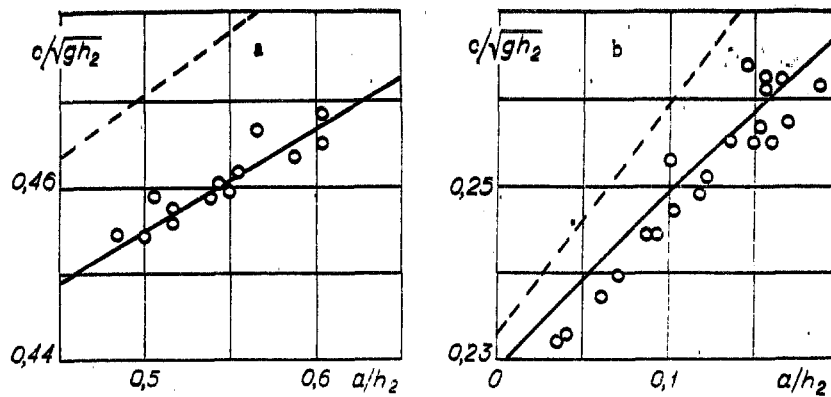


Fig. 3

pressed the Kelvin-Helmholtz instability in the experiments with the moving lower layer up to a difference in velocity of about 30 cm/sec, while in accordance with estimates made from the formulas given in [9] there was practically no effect on the characteristics of the sufficiently long solitary waves.

We consider the case of layers at rest in the unperturbed state. In accordance with [1, 3], the form of the solitary waves is then described by

$$\eta(x, t) = a \operatorname{sech}^2[k(x - ct)], \quad (1)$$

where k is wave number and t is time. Different formulas are given in [1, 3] correspondingly for the speed c :

$$c_1 = c_{10} \sqrt{1 + \frac{(m-1)a}{mh_2}} \sqrt{gh_2}; \quad (2)$$

$$c_2 = \left(c_{20} + \frac{\alpha a}{3h_2}\right) \sqrt{gh_2}, \quad (3)$$

where g is the acceleration due to gravity and c_{10} , c_{20} , and α are certain dimensionless quantities [1, 3], which are dependent on the density ratio σ and on the depth ratio $m = h_1/h_2$; the wave amplitude a , which governs not only c but also k , was considered as given.

The theoretical analysis [1, 3] shows that for certain values of σ and m only solitary waves can exist at the boundary with their convexity upwards ($a > 0$), while for other values there can only be waves with the convexity downwards ($a < 0$). At the free surface there is also a solitary wave in antiphase with the internal one and having a substantially smaller amplitude for the values of σ and m considered in the experiments. These theoretical results are qualitatively well confirmed in the experiments.

The check on (2) and (3) is illustrated by Figs. 2 and 3, where case a relates to waves with $a > 0$ and case b to ones with $a < 0$. In the first of these, we used all the experimental data in the range of m from 0.36 to 3.3 and a/h_2 from 0.04 to 0.6 with $\sigma = 0.8$. Along the abscissa we have the calculated values of the wave speed, while along the ordinate we have the experimental values c_e for the corresponding values of σ , m , and a/h_2 . If there were ideal correlation between the calculated and experimental data, the points in Fig. 2 would lie around a straight line representing the bisector of the coordinate angle. In fact, there is a certain systematic deviation, which is somewhat larger for points 2, which correspond to the model of [3], as against points 1, which correspond to the model of [1].

This deviation is not particularly large from the practical viewpoint, but it emphasizes a weak point in the mathematical models, which can be traced conveniently in [3], where the second approximation in shallow-water theory was used, but it was assumed that not one parameter was small but two (as these parameters one can take the ratio of the depth of the lower layer to the wave length and the ratio of the wave amplitude to the depth of the lower layer), and it was assumed that they both had the same order of smallness. The assumption that the first is small is important to deriving significant theoretical results, but solitary waves of very small amplitude are of substantially less practical interest, and it would be desirable to eliminate this constraint on the theory. A similar deficiency occurs in [1].

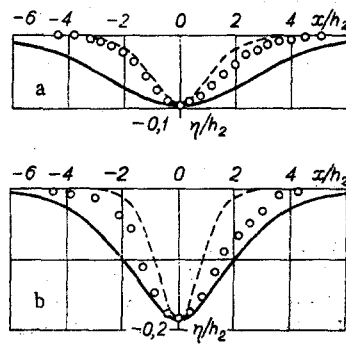


Fig. 4

In [8], no constraint was placed on the wave amplitude and, as is shown below, this results in substantially better agreement between the calculated and observed speeds.

A special experimental study is needed to determine what values of a/h_2 can be considered sufficiently small from the viewpoint of the models of [1, 3], since the upper bound to the smallness of this parameter is dependent in a complicated fashion on the values of σ and m , and also on the permissible discrepancy between the calculated and experimental values. Here we merely note that in this respect (2) had advantages over (3). To illustrate this, Fig. 3 shows the dependence of the wave speed on the amplitude with the following values of the parameters: $\sigma = 0.8$, $m = 3.3$, $h_2 = 0.92$ cm for Fig. 3a and $\sigma = 0.8$, $m = 0.357$, $h_2 = 3.5$ cm for Fig. 3b. In both cases, the solid lines have been obtained by calculation from (2) and the broken ones from (3), while the points show the experimental data.

Figure 4 compares the profiles of the solitary waves calculated from (1) and the experimental ones for $a < 0$, $\sigma = 0.8$, $m = 0.36$ and for the two values of a/h_2 given on the graphs. The calculations were based on the experimental value of a , since this parameter is considered as given in the theory as regards the scheme for these experiments. The solid lines correspond to the model of [1] and the broken lines to that of [3], while the experimental data are shown by the points. The best results as regards wave shape are given by the model of [3] for $a/h_2 = 0.1$. Then Figs. 2 and 3 indicate that the wave speed is not very much dependent on the profile, the amplitude being the more important parameter.

Figure 5 shows the paths of the liquid particles in the solitary wave in an immobile coordinate system, which was recorded by using particles of aluminum dust of size a few microns with $\sigma = 0.67$, $m = 3.5$, $h_2 = 1$ cm; the exposure time was 0.250 sec. The wave moved to the right and the horizontal projection of the particle velocities was directed to the left in the upper layer and to the right in the lower one. Distances between the divisions in the coordinate net engraved on the wall of the trough were 5 cm. One can clearly see the kinks in the particle paths at the interface, which indicates that the actual picture for the motion of the layers one with respect to the other corresponds closely to that used in the theoretical models.

When there is relative motion between the layers (Fig. 1b), the problem contains the further independent parameter $u = u_0/\sqrt{gH}$, which substantially extends the class of interesting phenomena but greatly complicates the examination. Here we give only restricted results designed to check the formula for the wave speed [8]:

$$c_3 = \frac{1-n}{1-\mu n} \left[u + \sqrt{u^2 - \frac{(u^2 - \mu n)(1 - \mu n)}{1-n}} \right] \sqrt{gH}, \quad (4)$$

where $n = h/H$; $\mu = 1 - \sigma$; when both layers are at rest,

$$c_4 = \sqrt{\frac{\mu n(1-n)}{1-\mu n}} \sqrt{gH}. \quad (5)$$

Theoretical analysis [8] also shows that there is a critical value for the depth of the unperturbed lower layer:

$$\frac{h_0^*}{H} = \frac{1 - u\sqrt{\sigma/\mu}}{1 - \sqrt{\sigma}}$$

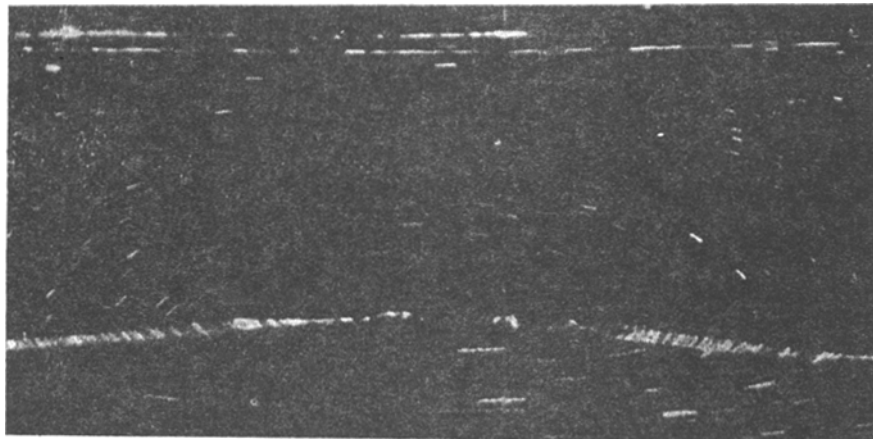


Fig. 5

TABLE 1.

H , cm	h_0 , cm	h_0/h_0^*	h , cm	u_0 , cm/sec	c_t , cm/sec	c_e , cm/sec
4	2,75	1,40	1,95	9,0	19,3	19,0
3,15	2,40	1,44	2,15	0	12,4	12,4
3,15	2,40	1,44	1,90	0	12,9	12,7
3,15	0,85	0,54	1,10	5,5	15,7	15,4
3,15	1,00	0,60	1,30	0	12,7	12,7
3,15	1,00	0,60	1,45	0	13,0	13,2

such that for $h_0 > h_0^*$ there can only be waves with $\alpha < 0$ and for $h_0 < h_0^*$ only with ones $\alpha > 0$.

Table 1 gives results from an experimental check on (4) and (5), in which the three top lines correspond to $h_0 > h_0^*$ and the three lower ones to $h_0 < h_0^*$; the last two columns give the experimental value c_e and the theoretical value c_t of the wave speed. There is good agreement, which is better than in the check on the models of [1, 3]. It should be noted that in the experiments with the moving lower layer, the solitary wave had a slightly unsymmetrical shape, for in the theory the wave is symmetrical. However, this does not lead to a discrepancy from the theoretical propagation speed, which agrees with what was said above.

As regards the effects of viscosity, one may note that it only produces weak wave damping. In the experiments on wave propagation in a liquid at rest it was found that the amplitude fell by about a factor e over a distance $s/l = 100$, where s is the path traveled and l is the length of the base of the rectangle having height a and area equal to the wave area. There was repeated reflection from the end walls of the trough.

We are indebted to L. V. Ovsyannikov for initiating these experiments and for considerable assistance.

LITERATURE CITED

1. G. H. Keulegan, "Characteristics of internal solitary waves," J. Res. of the Nat. Bur. of Stand., 51, No. 3 (1953).
2. A. S. Peters and J. J. Stoker, "Solitary waves in liquids having nonconstant density," Comm. Pure Appl. Math., 13, No. 1 (1960).
3. T. Kakutani and N. Yamasaki, "Solitary waves on the two-layer liquid," J. Phys. Soc. of Japan, 45, No. 2 (1978).
4. L. R. Walker, "Interfacial solitary waves in a two-fluid medium," Phys. Fluids, 16, No. 11 (1973).
5. C. G. Koop and G. Butler, "An investigation of internal solitary waves in a two-fluid medium," J. Fluid Mech., 112, 225 (1981).
6. R. E. Davis and A. Acrivos, "Solitary internal waves in deep water," J. Fluid Mech., 29, Pt. 3 (1967).

7. T. W. Kao and H.-P. Pao, "Wake collapse in the thermocline and internal solitary waves," *J. Fluid Mech.*, 97, Pt. 1 (1980).
8. L. V. Ovsyannikov, "The second approximation in shallow-water theory," *Izv. Akad. Nauk SSSR, Mekh. Zhid. Gaza*, No. 2 (1980).
9. S. A. Thorpe, "Experiments on the instability of stratified shear flows of immiscible fluids," *J. Fluid Mech.*, 39, Pt. 1 (1969).

CALCULATION OF THE ADJOINT MASSES FOR AN ANNULAR BLADE ASSEMBLY

L. A. Tkacheva

UDC 535.5:621.22

It is necessary to know the adjoint-mass coefficients in order to solve various problems in turbine aeroelasticity such as the calculation of the natural frequencies and forms of blade vibrations. These coefficients are known only for the planar set of plates [1-3], so interest attaches to estimating the effects of the three-dimensional flow on their magnitudes.

Here we consider the adjoint masses for a three-dimensional ring set of thin blades performing small harmonic oscillations with a constant phase shift in an incompressible fluid.

We use a cylindrical coordinate system r, θ, z for the ring set of N blades vibrating in a liquid between two unbounded cylinders C_1 and C_2 with radii r_1 and r_2 (Fig. 1). We assume that: 1) The liquid is ideal and incompressible and is at rest at infinity, while the flow is potential; 2) the blades are infinitely thin and represent screw surfaces defined by the equations

$$z = h(\theta - 2\pi n/N), \quad -\theta_0 < \theta - 2\pi n/N < \theta_0, \quad r_1 < r < r_2, \\ n = 0, 1, \dots, N-1,$$

where h the pitch of the screw surface and $2\theta_0$ the blade setting angle; 3) all the blades perform small oscillations with the same harmonic law but a certain phase shift $\mu = 2\pi n/N$, $n = 0, 1, \dots, N-1$.

We transfer to dimensionless coordinates r', θ', z' , referred to the characteristic length $L = r_2 - r_1$:

$$r' = r/L, \quad z' = z/L, \\ \theta' = \theta, \quad h' = h/L.$$

In what follows, the primes are omitted. By virtue of the third assumption, the vibration law can be put as

$$w^{(k)}(r, \theta, t) = Lf(r, \theta) \exp[i(k\mu + \omega t)],$$

where $w^{(k)}$ are the displacements of the points on blade k along the normal, ω is the circular frequency, and $f(r, \theta)$ is the dimensionless complex function that defines the form of the vibrations. We represent the velocity potential Φ in the form

$$\Phi = iL^2\omega\tilde{\Phi}(r, \theta, z) \exp(i\omega t).$$

Here $\tilde{\Phi}(r, \theta, z)$ is a dimensionless complex function that satisfies the Laplace equation

$$\Delta\Phi = 0 \tag{1}$$

and the following boundary conditions:

$$\lim_{|z| \rightarrow \infty} |\nabla\Phi| = 0; \tag{2}$$

$$\left. \frac{\partial\Phi}{\partial n} \right|_{S_k} = f(r, \theta) e^{ik\mu}, \quad k = 0, 1, \dots, N-1; \tag{3}$$